

Investigation of Coordination Ability of Mn(II), Fe(III), Co(II), Ni(II), and Cu(II) with Metronidazole, the Antiprotozoal Drug, in Alkaline Media: Synthesis and Spectroscopic Studies¹

F. A. I. Al-Khodir^a and M. S. Refat^{b,c*}

^aDepartment of Chemistry, College of Science,
Princess Nora Bint Abdul Rahman University, Riyadh, Saudi Arabia

^bDepartment of Chemistry, Faculty of Science, Port Said University, Port Said, Egypt

^cDepartment of Chemistry, Faculty of Sciences, Taif University,
Al-Haweiah, P.O. Box 888, Taif, 21974 Saudi Arabia

*e-mail: msrefat@yahoo.com

Received February 25, 2017

Abstract—Mn(II), Fe(III), Co(II), Ni(II), and Cu(II) complexes of metronidazole drug (Met) were synthesized in alkaline media at 60°C and characterized on the basis of elemental, molar conductance, magnetic, spectral (FT-IR, Raman, ESR, and solid reflectance), and thermal analyses. Metronidazole formed stable 1 : 2 molar ratio complexes with Mn(II), Co(II), Ni(II), and Cu(II). Fe(III) complex was obtained with 1 : 3 molar ratio. IR spectra of the solid complexes indicated that the Met drug behaved as a monodentate chelate through the oxygen atom of deprotonated –OH ethanol terminal group. According to the physical spectroscopic parameters (Racah repulsion, crystal field splitting, and nephelauxetic) and magnetic susceptibility, the complexes had an octahedral geometry, except Cu(II) complex that was square planar. Thermo gravimetric and differential thermo gravimetric analyses (TG–DTG) techniques demonstrated thermal degradation mechanisms of Met free drug and its metal complexes. Activation thermodynamic parameters, ΔE^* , ΔH^* , ΔS^* , and ΔG^* , were calculated for thermal decomposition steps of Met and its metal complexes.

Keywords: metronidazole, transition metals, chelation, thermal stability, Raman spectra

DOI: 10.1134/S107036321704034X

INTRODUCTION

Chemical structures of iron, cobalt, nickel, copper, zinc, and cadmium complexes are of high importance in biological systems [1–3]. Complexation of drug chelates or biochemical molecules with metal ions have significant influence on biochemical properties and bioavailability behavior in human cells [4].

Complexes of metal ions and imidazole moieties have been studied as radiosensitizers for tumor cells [5, 6]. Nitroimidazole drugs exhibited radiosensitizing activity that increased hypoxic cells sensibility to radiation and enhanced treatment efficiency in cancer radiotherapy in addition to a wide variety of other therapeutic properties [7, 8]. Metronidazole [Met, 2-(2-methyl-5-nitroimidazol-1-yl)ethanol] (Fig. 1) sensitizes

efficiently hypoxic cells to radiation induced damage. However, it shows toxicity in the clinical doses required for radiation therapy of cancer cells. Complexing ability of Met to Cu(II) was studied for gamma radiolysis and radiosensitization of thymine [9, 10]. Despite the extensive use of Met drug, only few papers have been published on its metal complexes [11–24] including its complexes with Co [11], Cu [11–16], Zn [11], Ru [17, 18], Rh [19, 20], Pd [15, 21, 22], Ag [23], and Pt [15, 24].

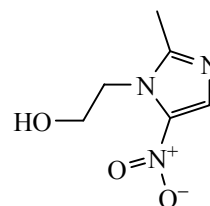


Fig. 1. Chemical structure of metronidazole drug (Met).

¹ The text was submitted by the authors in English.

Herein, we present the molecular structure of a metronidazole copper adduct that had not been previously observed. In continuation of our studies of metal-drugs interactions [25–27], we report interaction of metronidazole drug with Mn(II), Fe(III), Co(II), Ni(II), and Cu(II) ions in alkaline media.

EXPERIMENTAL

Metal salts (MnCl₂, FeCl₃, CoCl₂, NiCl₂·6H₂O, and CuCl₂) and metronidazole were purchased as “analytical” grade from Aldrich Chemical Company and the solvents used were absolute grade.

Preparation of metronidazole (Met) complexes.

Metronidazole (20 mmol, 3.43 g/mol) dissolved in 25 mL of methanol were mixed with 10 mmol of a Mn, Co, Ni, or Cu(II) chloride dissolved in distilled water (20 mL). The pH of the reaction mixture was adjusted to 7–8 by dilute ammonium hydroxide solution. A reaction mixture was refluxed for 30–45 min at 60°C. The colored solid complexes were filtered off, washed by absolute methanol and diethyl ether and dried in a desiccators over anhydrous CaCl₂·Fe(III) complex was prepared in accordance with the same procedure using 30 mmol of metronidazole (molar ratio Fe³⁺ : Met = 1 : 3).

Micro analyses was carried out on a Perkin Elmer CHN 2400 (USA) analyzer. Metals content was determined gravimetrically by converting the synthesized complexes to their stable oxide form. UV-Vis absorption spectra were recorded in nujol mull within 900–200 nm range on a UV2-Unicam UV-Vis Spectrophotometer. IR spectra (KBr discs) were recorded on a Bruker FT-IR Spectrophotometer. Raman spectra were recorded on a Bruker FT-Raman with laser 50 mW. Molar conductivity of all complexes of 10⁻³ mol/cm³ concentration in DMSO were measured on a Jenway 4010 conductivity meter. Magnetic measurements were carried out on a Sherwood Scientific magnetic balance using Gouy method with Hg[Co(CNS)₄] and [Ni(en)₃](S₂O₃) as solid calibrants. Their susceptibilities at 20°C were 16.44×10⁻⁶ and 11.03×10⁻⁶ c.g.s., decreasing by 0.05×10⁻⁶ and 0.04×10⁻⁶ per degree temperature raise respectively, at about room temperature. The cobalt compound, besides having the higher susceptibility, packed rather densely and was suitable for calibrating low fields, while the nickel compound with lower susceptibility and density was suitable for higher field. In that case Hg[Co(CNS)₄] was used as the calibrant. ESR spectrum of solid Cu(II) complex was measured on a Bruker EMX

Spectrometer (X-band 9.44 GHz) with 100 kHz modulation frequency. Microwave power was set at 1 mW and modulation amplitude was set at 4 Gauss. The low field signal was obtained after 4 scans with a 10 fold increase in the receiver gain. A powder spectrum was obtained in a 2 mm quartz capillary at room temperature. The thermal studies (TG–DTG) were carried out on a Shimadzu thermogravimetric analyzer at a heating rate of 10°C/min under the atmosphere of N₂.

All complexes were soluble in DMSO.

[Mn(Met)₂(NH₃)₂(H₂O)₂]·2H₂O. Yellow brown powder, yield 72%, *M* 501.35 g/mol. Found, %: C 28.43; H 6.00; N 22.13; Mn 10.91. C₁₂H₃₀N₈O₁₀Mn. Calculated, %: C 28.75; H 6.03; N 22.35; Mn 10.96.

[Fe(Met)₃(NH₃)₂(H₂O)]·5H₂O. Brown powder, yield 68%, *M* 708.44 g/mol. Found, %: C 30.22; H 5.87; N 21.65; Fe 7.62. C₁₈H₄₂N₁₁O₁₅Fe. Calculated, %: C 30.52; H 5.98; N 21.75; Fe 7.88.

[Co(Met)₂(NH₃)₂(H₂O)₂]·4H₂O. Violet powder, yield 71%, *M* 541.38 g/mol. Found, %: C 26.43; H 6.21; N 20.63; Co 10.78. C₁₂H₃₄N₈O₁₂Co. Calculated, %: C 26.62; H 6.33; N 20.70; Co 10.89.

[Ni(Met)₂(NH₃)₂(H₂O)₂]·4H₂O. Light green powder, yield 74%, *M* 541.14 g/mol. Found, %: C 26.52; H 6.30; N 20.60; Ni 10.77. C₁₂H₃₄N₈O₁₂Ni. Calculated, %: C 26.63; H 6.33; N 20.71; Ni 10.85.

[Cu(Met)₂(NH₃)₂]·4H₂O. Blue green powder, yield 76%, *M* 509.96 g/mol. Found, %: C 28.11; H 5.90; N 21.92; Cu 12.32. C₁₂H₃₀N₈O₁₀Cu. Calculated, %: C 28.26; H 5.93; N 21.97; Cu 12.46.

RESULTS AND DISCUSSION

Molar conductance values of the isolated solid complexes were measured in DMSO to be lower than 20 Ω⁻¹ cm² mol⁻¹ indicating their non-electrolytic nature.

IR spectra (Table 1) of Met complexes demonstrated similar bands due to the presence of the same chelate in all structures. Upon comparison of the spectrum of free Met and spectra of its complexes, the strong absorption band at 3219 cm⁻¹ in the spectrum of free Met was assigned to stretching O–H of the terminal ethanol group [28–31]. The band was overlapped with the band of the N–H bond in NH₃ and O–H stretching vibration of water molecules in the spectra of the complexes. Change in the intensity of O–H vibrations band confirmed that this group was a

Table 1. IR and Raman spectral data for Met drug and its complexes

Met	Compounds					Assignments
	Mn ²⁺	Fe ³⁺	Co ²⁺	Ni ²⁺	Cu ²⁺	
3219 (-)	3216 (3145)	3217 (3229)	3219 (-)	3218 (3205)	3221 (-)	$\nu(\text{OH}) + \nu(\text{NH})$
3096 (3102)	- (2977)	3098 (3098)	3098 (-)	3097 (3098)	3098 (-)	$\nu_{\text{as}}(\text{CH}_2)$
- (3019)	- (-)	- (3013)	- (-)	- (3023)	- (-)	$\nu_{\text{as}}(\text{CH}_3)$
2950, 2844 (2983, 2936)	2955 (2949)	2845 (2985, 2929)	2951 (-)	2953, 2845 (2976)	2952, 2846 (-)	$\nu_{\text{s}}(\text{CH}_2) + \nu_{\text{s}}(\text{CH}_3)$
1536 (1533)	1537 (1552)	1536 (1533)	1532 (-)	1536 (1533)	1537 (-)	$\nu_{\text{as}}(\text{NO}_2)$
1479 (1486)	1478 (1485)	1479 (1487)	1481 (-)	1479 (1487)	1479 (-)	$\nu(\text{C}=\text{N}) + \nu(\text{C}-\text{C})$
1429 (1467)	1424 (-)	1426 (-)	1427 (-)	1427 (-)	1428 (-)	$\delta(\text{CH}_2)$
1367 (1377)	1363 (1365)	1370 (1383)	1373 (-)	1369 (1365)	1367 (-)	$\delta(\text{CH}_3)$ def.
1267 (1268)	1264 (1261)	1268 (1271)	1267 (-)	1267 (1271)	1267 (-)	$\nu(\text{C}-\text{OH})$
1185 (1184)	1185 (1186)	1186 (1177)	1185 (-)	1185 (1177)	1186 (-)	CH_2 def.
1154 (1159)	1149 (-)	1156 (-)	1151 (-)	1155 (-)	1153 (-)	$\delta(\text{C}-\text{N}-\text{C})$
1075 (1075)	1064 (-)	1065 (1064)	1066 (-)	1064 (-)	1063 (-)	$\nu(\text{C}-\text{O})$
976, 906, 863 (991, 864)	987, 867 (-)	976, 906, 862 (970, 858)	999, 905 (-)	976, 906 (990, 859)	989, 905, 863 (-)	$\delta(\text{CH}_3) + \delta(\text{CH}_2)$
821 (828)	827 (830)	821 (820)	831 (-)	821 (820)	824 (-)	$\delta(\text{NO}_2)$
- (-)	564, 509 (568, 511)	557, 502 (549)	502 (-)	557, 501 (559, 503)	563, 502 (-)	$\nu(\text{M}-\text{O})$

chelation site of Met. The spectrum of Met had an absorption band at 1486 cm^{-1} due to stretching of C=C and C=N bonds [28–30]. The band was still remained at the same position of the spectra of the metal complexes. Such result indicated no coordination of nitrogen atom of imidazole ring in chelation process towards central metal ions. Two bands at 1535 and 826 cm^{-1} in the spectrum of Met were attributed to $\nu_{\text{as}}(\text{NO}_2)$ and $\delta(\text{NO}_2)$ vibrations of the nitro group [28, 30, 31]. These bands remained in the spectra of the metal complexes at the same wavenumbers, that

indicated no participation of the NO_2 group in the coordination. The strong band at 1074 cm^{-1} displayed by C–OH and C–O stretching in the Met ligand was shifted to lower frequency by $10\text{--}12 \text{ cm}^{-1}$ due to participation of –OH in coordination toward metal ions. The above data indicated coordination via oxygen of –OH terminal ethanol group after deprotonation.

Asymmetric stretching vibrations of the coordinated H_2O $\nu_{\text{as}}(\text{O}-\text{H})$ were assigned to the band of medium intensity at $3550\text{--}3380 \text{ cm}^{-1}$ while the

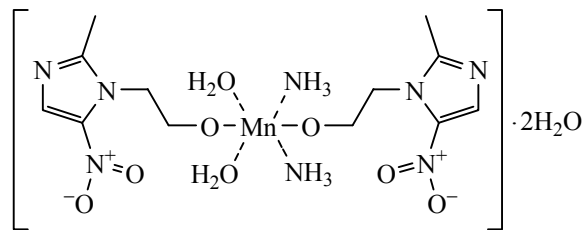


Fig. 2. Speculated structure of Mn(II) Met complex.

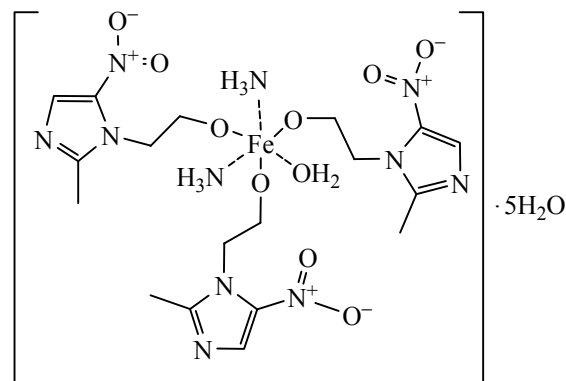


Fig. 3. Speculated structure of Fe(III) Met complex.

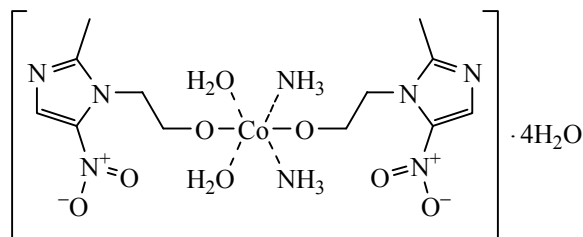


Fig. 4. Speculated structure of Co(II) Met complex.

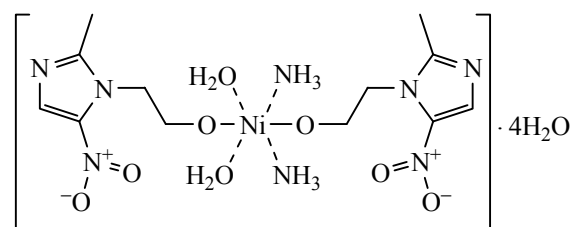


Fig. 5. Speculated structure of Ni(II) Met complex.

corresponding symmetric vibrations weak band was recorded at 3200–3100 cm^{-1} . The observation of only two bands vibrations for H_2O supported the molecular structure with only one molecule of water. The angular deformation motions of the coordinated water in the Met complexes could be classified into four types of vibrations: δ_b (bend), δ_r (rock), δ_t (twist), and δ_w (wag).

The most important vibration bands recorded in Raman spectra along with their assignments are given in Table 1. The accumulated data matched well with those of IR spectra and supported coordination of the ligand in its deprotonated form. Raman spectra for the Co(II) and Cu(II) complexes could not be recorded.

Solid reflectance, magnetic susceptibility and ESR. Solid reflectance spectrum of Mn(II) complex included three electronic bands at 16474, 28248, and 33003 cm^{-1} due to ${}^6A_{1g} \rightarrow {}^4E_{1g}$, ${}^4A_{1g}({}^4G)$, ${}^6A_{1g} \rightarrow {}^4E_g({}^4D)$, and ${}^6A_{1g} \rightarrow {}^4T_{1g}({}^4P)$ transitions [32]. The experimental magnetic moment value, 5.82 BM, was in good agreement with its high spin octahedral geometry (Fig. 2).

The diffuse reflectance spectrum of Fe(III) complex demonstrated two bands at 20618 and 28409 cm^{-1} that correspond to ${}^6A_{1g} \rightarrow {}^4T_{2g}$ (G) and ${}^6A_{1g} \rightarrow {}^4E_g$ (G) transitions, respectively in an octahedral geometry [33]. The magnetic moment value (5.71 BM) matched

with octahedral configuration around Fe(III) metal ion (Fig. 3).

Co(II) complex spectrum revealed solid reflectance transition bands at 22573 and 18622 cm^{-1} due to ${}^4T_{1g}(F) \rightarrow {}^4A_{2g}(F)$ (ν_3) and ${}^4T_{1g}(F) \rightarrow {}^4T_{1g}(P)$ (ν_2), respectively [32]. The experimental magnetic moment value was 4.94 BM. The calculated ligand field parameters ($\Delta q = 1384.2$, $B = 1010$, LFSE = 16610, and $\beta = 1.026$) [34] were in agreement with Co(II) octahedral geometry (Fig. 4).

The solid reflectance spectrum of Ni(II) complex displayed three transition bands at 27548 (ν_3), 16529 (ν_2), and 12136 (ν_1) cm^{-1} that correspond to ${}^3A_{2g}(F) \rightarrow {}^3T_{1g}(F)$, ${}^3T_{1g}(P) \rightarrow {}^3A_{2g}$ and ligand to metal charge transfer, respectively [32]. The ligand field parameters ($\Delta q = 1213.6$, $B' = 426$, $\beta = 0.41$, $\beta^0 = 58.90$, LFSE = 14563 and $\nu_2/\nu_1 = 1.362$) were estimated. The magnetic moment value was 6.31 BM, that corresponded to an octahedral structure [32] (Fig. 5).

The solid reflectance spectrum of the Cu(II) complex demonstrated a distinguish band at 16447 cm^{-1} due to ${}^2B_{1g} \rightarrow {}^2A_{1g}$ transition [32], also, another band at 28490 cm^{-1} could be assigned to the charge transfer transition. The magnetic moment (1.60 BM) value confirmed the square-planar geometry (Fig. 6).

The electron spin resonance spectrum of Cu(II)–Met complex (Table 2) made it evident that the unpaired electron was localized in the $d_{x^2 - y^2}$ orbital and the ground state was $^2B_{1g}$. The $g_{\parallel} < 2.3$ value confirmed the covalent character of the metal–ligand bond. The axial symmetry parameter, $G < 4$, indicated considerable exchange interaction in the solid complex [35], which was in agreement with the square planar geometry. In square planar complexes, the unpaired electron lies in the $d_{x^2 - y^2}$ orbital giving $g_0 > g_{\perp} > 2$ while the unpaired electron lies in the d_{z^2} orbital giving $g_{\perp} > g_{\parallel} > 2$.

Thermogravimetric and differential thermogravimetric analyses. The TG curve of metronidazole free drug demonstrated one thermal decomposition process at $DTG_{max} = 250^{\circ}C$, with completely mass loss 100% ($C_6H_9N_3O_3$) without a residue.

Thermograms of the Mn(II), Fe(III), Co(II), Ni(II), and Cu(II) metronidazole complexes exhibited the loss of uncoordinated and coordinated water, and NH_3 molecules within the temperature range of $50\text{--}200^{\circ}C$, and gradually decomposed to the corresponding metal oxides at higher temperatures. Presence of water molecules was also confirmed by the endothermic bands observed in the DTG curves, but the exothermic bands appeared at higher temperatures due to phase transition, oxidation or decomposition of the complex.

TG–DTG thermogram of $[Mn(Met)_2(NH_3)_2(H_2O)_2] \cdot 2H_2O$. The weight loss was measured in the range from room temperature to $900^{\circ}C$. The thermal decomposition process had three DTG_{max} stages at 100, 180, and $520^{\circ}C$. The first stage exhibited within the range of $50\text{--}120^{\circ}C$ was assigned to the loss of two uncoordinated water molecules (found: 7.50%; calculated: 7.18%). The second degradation stage occurred in the range of $120\text{--}210^{\circ}C$ due to loss of coordinated $2H_2O$ and $2NH_3$ molecules (found: 14.00%; calculated: 13.96%). The third degradation stage in the range of $210\text{--}900^{\circ}C$ was assigned to decomposition of two Met ligand molecules leaving MnO_2 as the final residue (found: 17.69%; calculated: 17.34%).

TG–DTG thermogram of $[Fe(Met)_3(NH_3)_3(H_2O)] \cdot 5H_2O$. The complex demonstrated two DTG_{max} stages at 180 and $470^{\circ}C$. The first stage exhibited within the range of $50\text{--}210^{\circ}C$ was assigned to the loss of one coordinated water molecule, five uncoordinated water molecules and two amino groups (found: 20.00%; calculated: 20.04%). Consequently, the second degradation stage occurred in the temperature range of 210--

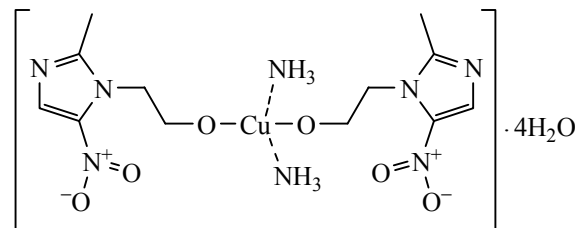


Fig. 6. Speculated structure of Cu(II) Met complex.

$900^{\circ}C$ and correspond to full decomposition and complete loss of three Met ligand molecules (found: 72.00%; calculated: 72.08%) leaving iron metal as the final residue (found: 8.00%; calculated: 7.88%).

TG–DTG thermogram of $[Co(Met)_2(NH_3)_2(H_2O)_2] \cdot 4H_2O$. The first stage ($50\text{--}300^{\circ}C$) was assigned to the loss of $4H_2O$ uncoordinated molecules, $2H_2O$ coordinated molecules and $2NH_3$ groups (found: 26.00%; calculated: 26.23%). Consequently, the second degradation stage ($300\text{--}900^{\circ}C$) correspond to full decomposition and complete loss of two Met ligand molecules (found: 55.00%; calculated: 55.50%) leaving CoO contaminated with two carbon atoms as a residual product (found: 19.00%; calculated: 18.27%).

TG–DTG of $[Ni(Met)_2(NH_3)_2(H_2O)_2] \cdot 4H_2O$. Thermal decomposition of the complex had two DTG_{max} stages at 210 and $570^{\circ}C$. The first stage ($50\text{--}280^{\circ}C$) was assigned to the loss of $4H_2O$ uncoordinated molecules, $2H_2O$ coordinated molecules and $2NH_3$ groups (found: 25.80%; calculated: 26.24%). Consequently, the second degradation stage ($280\text{--}900^{\circ}C$) correspond to full decomposition and complete loss of two Met ligand molecules (found: 60.70%; calculated: 59.96%) leaving NiO as the remaining product (found: 13.50%; calculated: 13.80%).

TG–DTG thermograms of $[Cu(Met)_2(NH_3)_2] \cdot 4H_2O$. The first stage ($50\text{--}250^{\circ}C$) was assigned to the loss of $4H_2O$ uncoordinated molecules and $2NH_3$ groups (found: 20.50%; calculated: 20.78%). Consequently, the second degradation stage ($250\text{--}900^{\circ}C$)

Table 2. The g parameter values for the Cu(II) complex

Parameter	Value
g_{\parallel}	2.2072
g_{\perp}	1.8071
g_0^a	1.9405

$$^a g_0 = (g_{\parallel} + 2g_{\perp})/3.$$

Table 3. Kinetic parameters determined using the Coats–Redfern (CR) and Horowitz–Metzger (HM) methods

Complex	Method	Parameter					<i>r</i>
		<i>E</i> *, kJ/mol	<i>A</i> , s ⁻¹	ΔS^* , J mol ⁻¹ K ⁻¹	ΔH^* , kJ/mol	ΔG^* , kJ/mol	
Met	CR	4.21×10 ⁴	1.20×10 ⁵	-1.44×10 ²	4.01×10 ⁴	2.10×10 ⁵	0.9840
	HM	3.99×10 ⁴	1.38×10 ⁶	-1.33×10 ²	3.33×10 ⁴	2.31×10 ⁵	0.9851
Mn(II)	CR	5.11×10 ⁵	2.21×10 ⁵²	-4.50×10 ²	5.01×10 ⁵	1.87×10 ⁵	0.9880
	HM	4.92×10 ⁵	5.77×10 ⁶¹	-3.43×10 ²	4.39×10 ⁵	1.54×10 ⁵	0.9591
Fe(III)	CR	2.96×10 ⁵	6.82×10 ⁴	-1.24×10 ²	4.32×10 ⁴	1.32×10 ⁵	0.9960
	HM	3.01×10 ⁵	5.01×10 ⁵	-1.30×10 ²	5.29×10 ⁴	1.34×10 ⁵	0.9892
Co(II)	CR	5.81×10 ⁵	8.02×10 ³	-1.73×10 ²	4.77×10 ⁴	1.38×10 ⁵	0.9611
	HM	6.21×10 ⁵	5.91×10 ⁴	-1.50×10 ²	5.43×10 ⁴	1.77×10 ⁵	0.9516
Ni(II)	CR	5.99×10 ⁵	5.11×10 ¹⁰	-4.31×10 ¹	4.31×10 ⁵	1.43×10 ⁵	0.9871
	HM	6.32×10 ⁵	3.30×10 ¹⁰	-2.46×10 ¹	5.38×10 ⁵	1.80×10 ⁵	0.9862
Cu(II)	CR	6.11×10 ⁵	4.88×10 ⁰⁹	-2.15×10 ¹	4.40×10 ⁵	1.28×10 ⁵	0.9896
	HM	6.23×10 ⁵	2.96×10 ¹⁰	-2.07×10 ¹	5.09×10 ⁵	1.35×10 ⁵	0.9866

corresponded to full decomposition and complete loss of two Met ligand molecules (found: 64.00%; calculated: 63.62%) leaving CuO oxide (found: 15.50%; calculated: 15.60%).

Calculations of the kinetic parameters. The TG–DTG curves obtained under conditions of non-isothermal decomposition were used for calculations of the kinetic parameters on the basis of the Coats–Redfern [36] and the modified Horowitz–Metzger [37] methods. The method of calculation in each case has already been reported.

The Coats–Redfern method. The order of the reaction was determined as described earlier by the use of the Coats–Redfern equation [36] from the plots:

$$\log [-\log (1 - \alpha)/T^2] \text{ vs } 1/T, \text{ for } n = 1, \quad (1)$$

$$\log [-\log (1 - \alpha)^{1-n}/T^2(1 - n)] \text{ vs } 1/T, \text{ for } n \neq 1, \quad (2)$$

where α is the fraction decomposed, n is the order of the reaction and T is the temperature (K). The activation energy (E^*) and the frequency factor (Z) were calculated from the slopes and intercepts, respectively, of the plots. The values E^* , Z , (ΔS^*), (ΔH^*), (ΔG^*), and correlation coefficient (r) are presented in Table 3.

The Horowitz–Metzger method. The TG–DTG curves were analyzed using the Horowitz–Metzger equation in the form:

$$\log [\log (1 - \alpha)^{-1}] = 100E\theta/2.3RT_i^2(T_f - T_i) - \log 2.3, \quad (3)$$

where T_i is the temperature of inception of the reaction, T_f is the temperature of completion of the reaction, θ is the difference between the temperature at inflection point of the thermogram (T_s) and the temperature under consideration, and R is the gas constant. A plot of the left-hand side of Eq. (3) vs θ was linear as required by the theory and E was calculated from the slope.

The activation enthalpy (ΔH^*), the activation entropy (ΔS^*) and the free energy of activation (ΔG^*) were calculated (Table 3) using the following equations:

$$\Delta S^* = 2.303[\log (Zh/KT)]R, \quad (4)$$

$$\Delta H^* = E - RT, \quad (5)$$

$$\Delta G^* = \Delta H^* - T_s \Delta S^*, \quad (6)$$

where Z , K , and h are the pre-exponential factor, Boltzman, and Plank constants, respectively [38].

In the overview on the kinetic data deduced from TG–DTG curves, it was found that all Met complexes had negative values for the entropy parameter indicating that activated complexes had more ordered systems than reactants [38]. The activation energy (E^*) values of Mn(II), Co(II), and Ni(II) complexes had almost the same thermal stability due to their *iso*-structure.

REFERENCES

1. Bakirdere, E.G., Fellah, M.F., Canpolat, E., Kaya, M., and Gür, S., *J. Serb. Chem. Soc.*, 2016, vol. 81, p. 509. doi 10.2298/JSC151030008B

2. Terenzi, A., Pirker, C., Keppler, B.K., and Berger, W., *J. Inorg. Biochem.*, 2016, vol. 165, p. 71. doi 10.1016/j.jinorgbio.2016.06.021
3. Sharma, S., Chauhan, M., Jamsheera, M., Tabassum, S., and Arjmand, F., *Inorg. Chim. Acta*, 2017, vol. 458, p. 8. doi 10.1016/j.ica.2016.12.011
4. Tahghighi, A., *J. Organomet. Chem.*, 2014, vol. 770, p. 51. doi org/10.1016/j.jorganchem.2014.08.007
5. Farrel, N., *Prog. Clin. Biochem. Med.*, 1989, vol. 10, p. 89.
6. Ramalho, T.C., Buhi, M., Figueroa-Villar, J.D., and Alencastro, R.B., *Helv. Chim. Acta*, 2005, vol. 88, p. 2705. doi 10.1002/hlca.200590210
7. Kapoor, V.K., Chadha, R., Venissety, P.K., and Prasanth, S., *J. Sci. Ind. Res.*, 2003, vol. 62, p. 659.
8. Raether, W. and Hanel, H., *Parasitol. Res.*, 2003, vol. 90, p. S19.
9. Mandal, P.C., Bardhan, D.K., and Bhattacharyya, S.N., *Bull. Chem. Soc. Jpn.*, 1990, vol. 63, p. 2975. doi 10.1246/bcsj.63.2975.
10. Roy, M.B., Mandal, P.C., and Bhattacharyya, S.N., *Int. J. Radiat. Biol.*, 1996, vol. 69, p. 471. doi 10.1080/095530096145760
11. Galvan-Tejada, N., Bernes, S., Castillo-Blum, S.E., Noth, H., Vicente, R., and Barba-Behrens, N., *J. Inorg. Biochem.*, 2002, vol. 91, p. 339. doi 10.1016/S0162-0134(02)00468-3
12. Barba-Behrens, N., Mutio-Rico, A.M., Joseph-Nathan, P., and Contreras, R., *Polyhedron*, 1991, vol. 10, p. 1333. doi 10.1016/S0277-5387(00)81266-8
13. Athar, F., Husain, K., Abid, M., Agarwal, S.M., Coles, S.J., Hursthouse, M.B., Maurya, M.R., and Azam, A., *Chem. Biodivers.*, 2005, vol. 2, p. 1320. doi 10.1002/cbdv.200590104
14. Ratajczak-Sitarz, M., Katrusiak, A., Wojakowska, H., Januszczuk, M., Krzyminiowski, R., and Pietrzak, R., *J. Inorg. Chim. Acta*, 1998, vol. 269, p. 326.
15. Bharti, N., Shailendra, Coles, S.J., Hursthouse, M.B., Mayer, T.A., Garza, M.T.G., Cruz-Vega, D.E., Mata-Cardenas, B.D., Naqvi, F., Maurya, M.R., and Azam, A., *Helv. Chim. Acta*, 2002, vol. 85, p. 2704. doi 10.1002/1522-2675(200209)85:9<2704::AID-HLCA2704>3.0.CO;2-X
16. (a) Zheltvai, O.I., Zheltvai, I.I., Spinul, V.V., and Antonovich, V.P., *J. Anal. Chem.*, 2013, vol. 68, p. 600. doi 10.1134/S1061934813050171. (b) Valderrama-Negron, A.C., Alves, W.A., Cruz, A.S., Rogero, S.O., and Silva, D.D., *Inorg. Chim. Acta*, 2011, vol. 367, p. 85. doi 10.1016/j.ica.2010.12.006
17. Wu, A., Kennedy, D.C., Patrick, B.O., and James, B.R., *Inorg. Chem.*, 2003, vol. 42, p. 7579. doi 10.1021/ic030119j.
18. Kennedy, D.C., Wu, A., Patrick, B.O., and James, B.R., *J. Inorg. Biochem.*, 2006, vol. 100, p. 1974. doi 10.1016/j.jinorgbio.2006.07.001.
19. Dyson, T.M., Morrison, E.C., Tocher, D.A., Dale, L.D., and Edwards, D.I., *Inorg. Chim. Acta*, 1990, vol. 169, p. 127. doi 10.1016/S0020-1693(00)82045-9
20. Nothenberg, M.S., Zyngicr, S.B., Giesbrecht, A.M., Gambardella, M.T.P., Santos, H.A., Kimura, E., and Najjar, R., *J. Braz. Chem. Soc.*, 1994, vol. 5, p. 23. doi org/10.5935/0103-5053.19940005
21. De Bondt, H.L., Blaton, N.M., Peeters, O.M., and De Ranter, C.J., *Acta Cryst. C*, 1994, vol. 50, p. 180. doi 10.1107/S0108270193006882
22. Rochon, F.D., Melanson, R., and Farrell, N., *Acta Cryst. C*, 1993, vol. 49, p. 1703. doi 10.1107/S0108270193002537
23. Fun, H.K., Jebas, S.R., and Balasubramanian, T., *Acta Cryst. E*, 2008, vol. 64, p. M668. doi 10.1107/S1600536808009860
24. Bales, J.R., Coulson, C.J., Gilmour, D.W., Mazid, M.A., Neidle, S., Kuroda, R., Peart, B.J., Ramsden, C.A., and Sadler, P.J., *J. Chem. Soc. Chem. Commun.*, 1983, vol. 8, p. 432. doi 10.1039/C39830000432
25. Alghamdi, M.T., Alsibaai, A.A., Shahawi, M.S., and Refat, M.S., *J. Mol. Liq.*, 2016, vol. 224, p. 571. doi 10.1016/j.molliq.2016.10.038
26. Refat, M.S., El-Megharbel, S.M., Hussien, M.A., Hamza, R.Z., Al-Omar, M.A., Naglah, A.M., Afifi, W.M., and Kobeasy, M.I., *Spectrochimica Acta Part C*, 2017, vol. 173, p. 122. doi 10.1016/j.saa.2016.08.053
27. Alghamdi, M.T., Alsibaai, A.A., Shahawi, M.S., and Refat, M.S., *J. Mol. Struct.*, 2017, vol. 1130, p. 264. doi 10.1016/j.molstruc.2016.10.036
28. Nakamoto, K., *Infrared and Raman Spectra of Inorganic and Coordination Compounds*, 5th ed., New York: John Wiley and Sons, Inc., 1997.
29. Carter, D.A. and Pemberton, J.E., *J. Raman Spectrosc.*, 1997, vol. 28, p. 939.
30. Masciocchi, N., Bruni, S., Cariati, E., Cariati, F., Galli, S., and Sironi, A., *Inorg. Chem.*, 2001, vol. 40, p. 5897. doi 10.1021/ic010384+
31. Lever, A.B.P., *Crystal Field Spectra Inorganic Electronic Spectroscopy*, 1st ed., Elsevier, Amsterdam, 1968, p. 249.
32. Anuradha, S. and Pramila, S., *Indian. J. Chem.*, 2000, vol. 39A, p. 874.
33. Centre, P.G., Nareda, T.G., and Murthy, B.N., *Indian J. Chem.*, 1989, vol. 28A, p. 689.
34. Griffith, J.S., *The Theory of Transition Metals Ions*, Cambridge University Press, 1961.
35. Coats, A.W. and Redfern, J.P., *Nature*, 1964, vol. 201, p. 68. doi 10.1038/201068a0
36. Horowitz, H.H. and Metzger, G., *Anal. Chem.*, 1963, vol. 35, p. 1464. doi 10.1021/ac60203a013
37. Olszak-Humienik, M. and Mozejko, J., *Thermochimica Acta*, 2000, vol. 344, p. 73.